CHEMISTRY
A EUROPEAN JOURNAL

DOI: 10.1002/chem.200902453

Secondary Interactions or Ligand Scrambling? Subtle Steric Effects Govern the Iridium(I) Coordination Chemistry of Phosphoramidite Ligands

Tina Osswald, Heinz Rüegger†, and Antonio Mezzetti*[a]

Abstract: The *like* and *unlike* isomers of phosphoramidite (P*) ligands are found to react differently with iridium(I), which is a key to explaining the apparently inconsistent results obtained by us and other research groups in a variety of catalytic reactions. Thus, the *unlike* diastereoisomer (*aR*,*S*,*S*)-[IrCl(cod)(**1a**)] (**2a**; cod = 1,5-cyclooctadiene, **1a** = (*aR*,*S*,*S*)-(1,1′-binaphthalene)-2,2′-diyl bis(1-phenylethyl)phosphoramidite) forms, upon chloride abstraction, the monosubstituted complex (*aR*,*S*,*S*)-[Ir(cod)(1,2-η-**1a**,κP)]$^+$ (**3a**), which contains a chelating P* ligand that features an η^2 interaction between a dangling phenyl group and iridium. Under analogous conditions, the *like* analogue (*aR*,*R*,*R*)-**1a′** gives the disubstituted species (*aR*,*R*,*R*)-[Ir(cod)(**1a′**,κP)$_2$]$^+$ (**4a′**) with monodentate P* ligands. The structure of **3a** was assessed by a combination of X-ray and NMR spectroscopic studies, which indicate that it is the configuration of the binaphthol moiety (and not that of the dangling benzyl N groups) that determines the configuration of the complex. The effect of the relative configuration of the P* ligand on its iridium(I) coordination chemistry is discussed in the context of our preliminary catalytic results and of apparently random results obtained by other groups in the iridium(I)-catalyzed asymmetric allylic alkylation of allylic acetates and in rhodium(I)-catalyzed asymmetric cycloaddition reactions. Further studies with the *unlike* ligand (*aS*,*R*,*R*)-(1,1′-binaphthalene)-2,2′-diyl bis{[1-(1-naphthalene-1-yl)ethyl]phosphoramidite} (**1b**) showed a yet different coordination mode, that is, the η^4-arene–metal interaction in (*aS*,*R*,*R*)-[Ir(cod)(1,2,3,4-η-**1b**,κP)]$^+$ (**3b**).

Keywords: asymmetric catalysis · chirality · diastereoselectivity · iridium · ligand effects

Introduction

The introduction of chiral phosphoramidite ligands (P*) has generated a revival of monodentate ligands and a burst of applications in asymmetric catalysis.[1] Several aspects concerning these ligands are still unclear, though. Interestingly, a number of investigations have shown that P* ligands do not always act as monodentate. Thus, iridium complexes of methylamino-substituted P* ligands readily undergo C–H activation and give cyclometalated complexes with P,CH_2 bidentate coordination that efficiently catalyze enantioselective allylic alkylation and amination.[2–4] Also, the substituents at the nitrogen atom have been recognized to be noninnocent, but their effects are poorly understood.[5] For instance, the *unlike* and *like* diastereomeric ligands (*aR*,*S*,*S*)-**1a** and (*aR*,*R*,*R*)-**1a′** show widely differing influences in the iridium(I)-catalyzed asymmetric allylic alkylation of allylic acetates,[6] as well as in the rhodium(I)-catalyzed asymmetric [5+2] cycloaddition of alkyne-vinylcyclopropanes.[7]

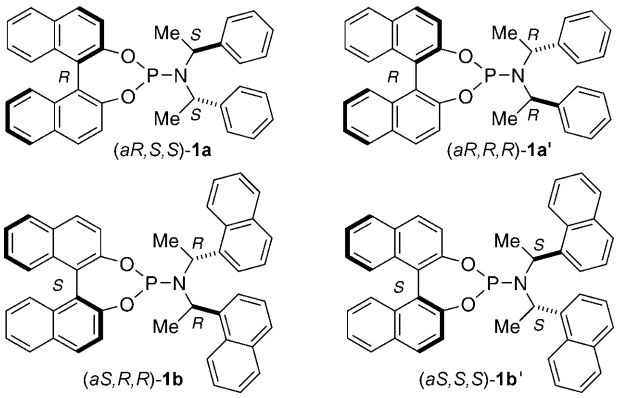

[a] T. Osswald, Dr. H. Rüegger, Prof. Dr. A. Mezzetti
Department of Chemistry and Applied Biosciences
ETH Zürich, ETH Hönggerberg
8093 Zürich (Switzerland)
Fax: (+41) 44-632-6121
E-mail: mezzetti@inorg.chem.ethz.ch

[†] Deceased June 28, 2009.

Supporting information for this article is available on the WWW under http://dx.doi.org/10.1002/chem.200902453.

After our discovery that dangling aryl groups on the phosphoramidite nitrogen atom give an η^2 interaction with a 16-electron metal fragment, as in the d^6 half-sandwich complex (aS,S_{Ru},R_C,R_C)-[RuCl(η^6-*p*-cymene)(1,2-η-Ph-**1b**-κP)]$^+$ (**5**),[8]

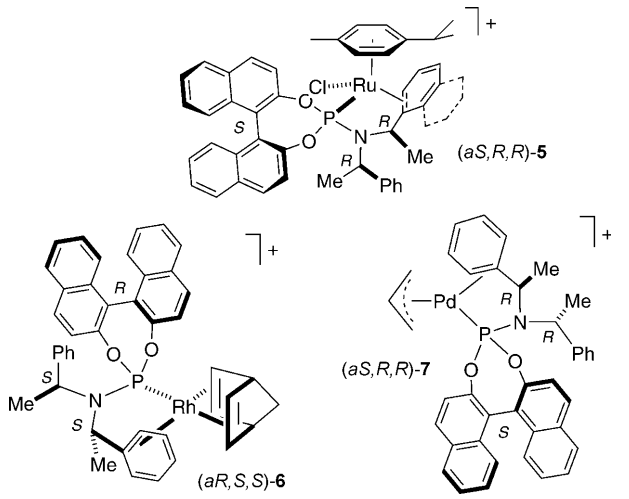

we started a systematic study of the topic. Thus, we have recently reported the square-planar d^8 cationic species (aS,R,R)-[Pd(η^3-allyl)(1,2-η-Ph-**1a**-κP)]$^+$ (**7**) and (aR,S,S)-[Rh(nbd)(1,2-η-Ph-**1a**-κP)]$^+$ (**6**; nbd = norbornadiene).[9]

In general, secondary interactions between the metal and bulky aryl substituents of the phosphine ligands have been recently recognized to play an important role in catalysis.[10] In particular, they are pivotal in complexes of Pd^{II},[11–13] Pd^0,[14] and Pd^I,[15] which catalyze enantioselective C–C bond-forming reactions. Such effects have not yet been systematically exploited, and we believe that their study will have far-reaching consequences in catalysis. In the present study, we show that secondary interactions dramatically depend on the relative configuration of the axial and central stereogenic elements of the P* ligands and on the nature of the arene appendage.

During a preliminary screening of the asymmetric cyclopropanation of olefins catalyzed with complexes of the type [MCl(cod)(P*)] (M = Rh or Ir, cod = 1,5-cyclooctadiene) as precatalysts, we were intrigued by the fact that the results obtained with the *like* and *unlike* diastereoisomers of the P* ligands showed no clear-cut trend. This prompted us to examine the iridium(I) coordination chemistry with both the *like* and *unlike* diastereoisomers of the P* ligands (aR,S,S)-**1a**, (aR,R,R)-**1a′**, (aS,R,R)-**1b**, and (aS,S,S)-**1b′**. In our previous investigations of d^8 Pd^{II} and Rh^I complexes, we always used the *unlike* diastereoisomers of the P* ligands, that is, ligands (aR,S,S)-**1a** or (aS,R,R)-**1b**.

Thereby, we discovered that the secondary interactions between the metal and the chiral *N*-benzyl substituents in cationic iridium(I) complexes are highly sensitive to subtle steric and electronic effects, and in particular to the relative configuration of the axial and central stereogenic elements of the P* ligands and the nature of the arene appendage.

Results and Discussion

[IrCl(cod)(P*,κP)]: The complexes (aR,S,S)-[IrCl(cod)(**1a**)] (**2a**), (aR,R,R)-[IrCl(cod)(**1a′**)] (**2a′**), (aS,R,R)-[IrCl(cod)-(**1b**)] (**2b**), and (aS,S,S)-[IrCl(cod)(**1b′**)] (**2b′**) were prepared by reaction of $[MCl(cod)]_2$ with the ligand (2 equiv) in dichloromethane at room temperature and fully characterized (Scheme 1).

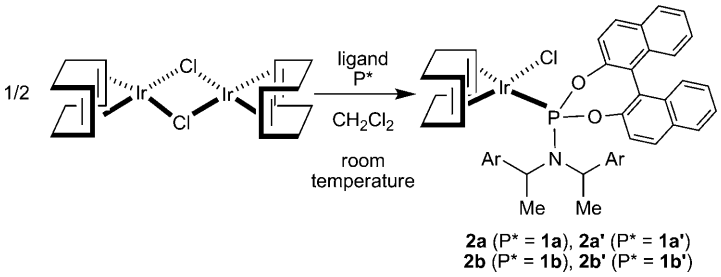

Scheme 1. Synthesis of the neutral complexes [IrCl(cod)(P*)].

Complexes (aR,S,S)-**2a** and (aS,S,S)-**2b′** crystallized from diethyl ether as orange platelets and red needles, respectively, and were studied by X-ray diffraction. As the structural data of **2a** and **2b′** are very similar, they will be discussed together. Both complexes exhibit a fairly regular square-planar coordination (Figure 1) with similar metrical parameters (Table 1), the most evident difference being the confor-

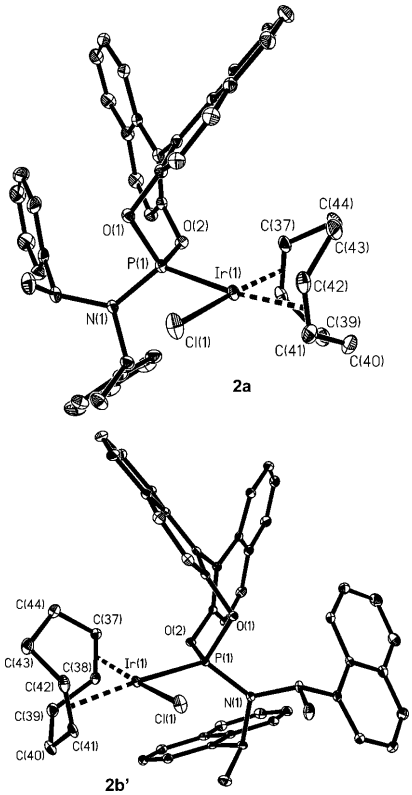

Figure 1. ORTEP plots of (aR,S,S)-[IrCl(cod)(**1a**,κP)] (**2a**) and (aS,S,S)-[IrCl(cod)(**1b**,κP)] (**2b′**).

Table 1. Selected bond lengths [Å] and angles [°] for (*aR*,*S*,*S*)-**2a**, (*aS*,*S*,*S*)-**2b′**, and **6**.[9]

	(*aR*,*S*,*S*)-**2a**	(*aS*,*S*,*S*)-**2b′**	**6**[9]
M–P	2.2503(5)	2.2687(6)	2.2481(7)
M–Cl	2.3459(5)	2.3487(7)	2.3499(8)
M–C(37)	2.129(2)	2.099(3)	2.137(3)
M–C(38)	2.121(2)	2.130(3)	2.124(3)
M–C(41)	2.243(2)	2.217(2)	2.270(3)
M–C(42)	2.222(2)	2.232(3)	2.243(3)
C1-M-C(37)	161.21(6)	150.78(8)	161.04(8)
Cl-M-C(38)	158.82(6)	167.70(7)	159.89(8)
C1-M -C(41)	92.04(7)	89.13(8)	93.05(9)
Cl-M-C(42)	88.23(7)	87.77(8)	88.84(9)
P-M-C(37)	93.51(6)	93.71(7)	94.22(8)
P-M-C(38)	94.63(7)	95.11(7)	94.28(9)
P-M-C(41)	170.13(7)	157.58(8)	169.68(9)
P-M-C(42)	153.93(6)	166.33(8)	155.27(9)
P-M-Cl	89.63(2)	91.46(2)	88.53(3)
C(37)-M-C(41)	88.04(9)	96.7(1)	96.7(1)
C(38)-M-C(42)	96.69(9)	88.3(1)	96.6(1)

mation adopted by the phosphoramidite. Indeed, **2a** and **2b′**, which feature opposite binaphthol configurations but the same configuration at the phenethyl moiety (*S*), assume pseudo-enantiomeric conformations. Therefore, the conformation is determined by the binaphthyl moiety in these complexes, whereas the configuration of the central stereogenic elements (the phenethyl substituents at nitrogen) is—at this stage—irrelevant.

The Ir–P distances are similar to those observed in other phosphoramidite complexes of the type [IrCl(cod)(P*)] (2.236(1)–2.265(3) Å),[16] as well as in the rhodium analogue (*aS*,*R*,*R*)-[RhCl(cod)(**1a**,κP)] (**6**; 2.2481(7) Å).[9] In contrast, the metal–olefin bonds, in particular those *trans* to P, are shorter in the iridium complex **2a** than in the rhodium analogue **6** according to a trend that is found in other olefin complexes of rhodium(I) and iridium(I).[17,18] As a consequence, the tetrahedral distortion of the square-planar geometry, which is present in all three [MCl(cod)(P*)] complexes, is larger in the iridium(I) complexes, as the short Ir–olefin distance enhances the steric interactions between cod and the other ligands. The dihedral angles between the P–Ir–Cl plane and the plane defined by the centroids of the olefin bonds and the metal atom are 8.2° (**2a**), 10° (**2b′**), and 7.2° (**6**).

The asymmetry of the binding of the diolefin is similar in (*aR*,*S*,*S*)-**2a** and **6** (0.13 and 0.11 Å, respectively) and, overall, larger than in phosphine complexes of the type [MCl(cod)(PPh_2R)] (R = aryl), for which the difference between the average M–olefin distances *trans* to P and to Cl are 0.7 (Rh)[17] and 0.6 Å (Ir),[18] respectively. The longer metal–olefin distances *trans* to the P donor reflect the greater competition for the π electrons between the olefin and the P ligand, which is larger with the more π-acidic phosphoramidites than with phosphines. This results from the increased electronegativity of the P substituents on going from the carbon in PPh_3 to nitrogen and oxygen in phosphoramidites.

Next, we studied the chloride abstraction reaction from the neutral chloro complexes of the type [IrCl(cod)(P*,κP)] containing the four P* ligands under investigation with $AgSbF_6$ as scavenger, and determined the solution structure of all products by multinuclear NMR spectroscopy. As expected by analogy with the rhodium derivative (*aR*,*S*,*S*)-**6**,[9] chloride abstraction from the *unlike* derivative (*aR*,*S*,*S*)-[IrCl(cod)(**1a**,κP)] (**2a**) gives (*aR*,*S*,*S*)-[Ir(cod)(1,2-η-**1a**,κP)]$^+$ (**3a**; Scheme 2).

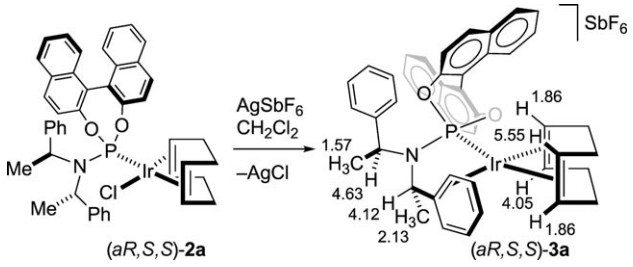

Scheme 2. The *unlike* ligand **1a** gives monosubstituted complex **3a**.

NMR spectroscopic studies of (*aR*,*S*,*S*)-3a: The key ^{13}C NMR signals of the Ir-bound phenyl group were located by a combination of NMR spectroscopic methods (^{31}P–^1H HMQC, ^{13}C–^1H HMQC, ^{13}C–^1H HMBC, ^1H–^1H COSY, and ^1H–^1H ROESY) at −80 °C as described below. Further details, as well as the relevant NMR spectra, are reported in the Supporting Information.

The ^1H NMR spectrum of (*aR*,*S*,*S*)-**3a** is temperature dependent. In particular, the signals of a phenyl ring are broad at room temperature and sharpen up at −80 °C. This indicates that the dynamic process, which is most probably the hindered rotation of the η^2-coordinated phenyl ring, is slowed down but not completely frozen at −80 °C. At this temperature, the ^1H NMR spectrum exhibits a broad, but resolved, signal for one proton at an unusually low frequency ($\delta = 6.57$ ppm, Figure S2a in the Supporting Information), which is indicative of an η^2 interaction between iridium and the phenyl ring.[9] This signal was assigned to an *ortho* H atom by determination of the connectivity within the phenyl ring with a ROESY experiment (Supporting Information, Figure S4).

A short-range ^{13}C–^1H HMQC experiment (Supporting Information, Figure S3) revealed the one-bond connectivity to the *ortho* C atom at $\delta = 96.2$ ppm, which is shifted to low frequency (Scheme 3). This feature is diagnostic of an η^2-

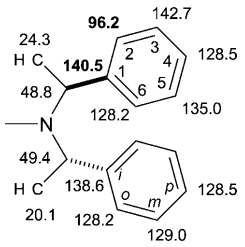

Scheme 3. ^{13}C NMR chemical shifts of the $N(CH(Me)Ph)_2$ moiety of (*aR*,*S*,*S*)-**3a** (metal-bonded C atoms in boldface; CD_2Cl_2, 233 K).

arene–metal interaction, as well as the high-frequency shift affecting one *meta* C atom (Supporting Information, Figure S3).[9,19] The signal of the *ipso* C atom was found at $\delta =$ 140.5 ppm by a long-range ^{13}C–^{1}H HMBC experiment. This value is slightly shifted to high frequency, which is again typical for phenyl rings involved in an η^2 interaction.[19]

The cod vinyl signals were assigned by means of a ROESY experiment (Supporting Information, Figure S4) and the ^{1}H NMR spectrum. The vicinal H atoms resonating at $\delta = 1.86$ and 5.55 ppm belong to the double bond *trans* to the P* ligand, as indicated by their coupling to phosphorus ($^{3}J_{P,H} = 10.2$ and 8.1 Hz, respectively; Supporting Information, Figure S2b). The lack of resolved P,H coupling for the vinylic H atoms that resonate at $\delta = 1.86$ and 4.15 ppm indicates a *cis* relationship to the P* ligand.

The activation energy for the phenyl rotation is only 4.3 kcal mol^{-1} (see Experimental Section), which indirectly suggests that the η^2 interaction is weak. For reference, a DFT study of the d^8 complex (*aS*,*R*,*R*)-[Pd(η^3-allyl)(**1a**)]$^+$ (**7**) suggests that the energy involved in the η^2-arene–metal interaction in **7** is as low as ~13 kcal mol^{-1},[9] whereas a much higher value (30 kcal mol^{-1}) resulted for the d^6 complex (*aS*,*R*,*R*)-[RuCl(η^6-*p*-cymene)(1,2-η-Ph-**1b**-κP)]$^+$ (**5**).[19]

(*aR*,*R*,*R*)-[Ir(cod)(1,2-η-1a′,κP)]$^+$ (4a′): Under the same conditions as those used for (*aR*,*S*,*S*)-**2a**, the diastereoisomeric (*aR*,*R*,*R*)-[IrCl(cod)(**1a′**)] (**2a′**) reacted with $AgSbF_6$ (1 equiv) to give the disubstituted cation (*aR*,*R*,*R*)-[Ir(cod)-(**1a′**,κP)$_2$]$^+$ (**4a′**, 0.5 equiv; Scheme 4) instead of a complex featuring an η^2 interaction.

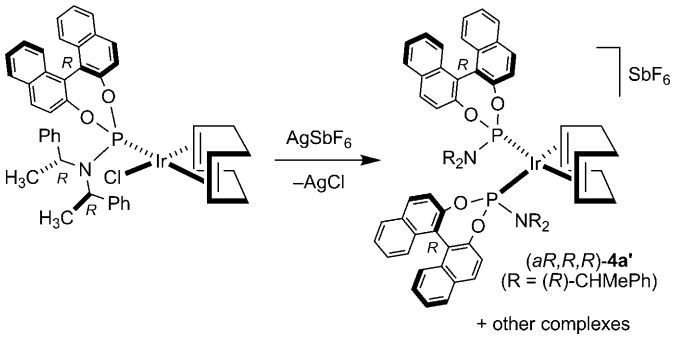

Scheme 4. The *like* diastereoisomer (*aR*,*R*,*R*)-**1a′** gives the disubstituted iridium(I) cationic complex **4a′** by ligand scrambling.

The formulation of **4a′** is suggested by the ^{1}H and ^{13}C NMR spectra. In particular, the ^{1}H NMR spectrum shows only two olefinic proton signals at $\delta = 5.37$ and 3.61 ppm, which indicates that the complex is C_2-symmetric (Supporting Information, Figure S9). It should be noted that the ^{31}P NMR spectrum (Supporting Information, Figure S8) is not diagnostic for two reasons. First, the two equivalent P atoms give a singlet just as a monosubstituted complex would. Furthermore, the chemical shift of $\delta = 132.2$ ppm is unexceptional if compared with the value of $\delta = 118.4$ ppm found for (*aR*,*S*,*S*)-**3a**.

To substantiate that it is chloride abstraction that triggers the ligand scrambling, we treated [IrCl(cod)]$_2$ with the *like* diastereoisomer (*aR*,*R*,*R*)-**1a′** (4 equiv) in CD_2Cl_2. The ^{1}H and ^{31}P NMR spectra of the reaction solution showed the signals of the monosubstituted complex (*aR*,*R*,*R*)-**2a′** and of unreacted **1a′** in a 1:1 ratio (Scheme 5). Addition of $AgSbF_6$ (1 equiv) gave the disubstituted complex **4a′**.

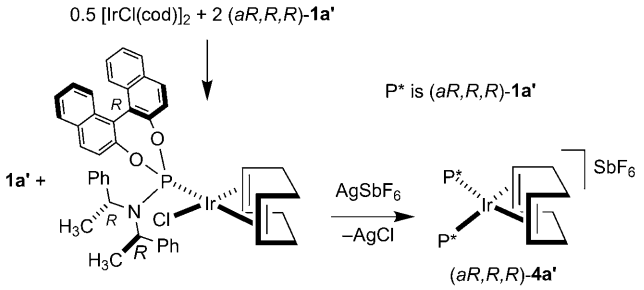

Scheme 5. The stepwise synthesis of (*aR*,*R*,*R*)-**4a′** shows that the ligand scrambling takes place after chloride abstraction.

Ligand scrambling to give the disubstituted species **4a′** takes place *after* addition of $AgSbF_6$ (1 equiv versus Ir) to the reaction solution, which indicates that **4a′** is more stable than the hypothetical η^2-arene complex [Ir(cod)(1,2-η-**1**,κP)]$^+$. As the only difference between the neutral chloro complexes (*aR*,*S*,*S*)-**2a** and (*aR*,*R*,*R*)-**2a′** is the relative configuration of the axial and central stereogenic elements of the phosphoramidite ligand, we studied the effect of changing the relative configuration at the phenethyl moiety in [Ir-(cod)(1,2-η-P*,κP)]$^+$ by molecular modeling (MM). MM calculations of the *unlike* and *like* diastereoisomers of [Ir-(cod)(1,2-η-P*,κP)]$^+$ showed that the complex with the *like* *aR*,*R*,*R* ligand would be less stable (by 6.3 kcal mol^{-1}) than the experimentally observed (*aR*,*S*,*S*)-**3a** (Scheme 6).

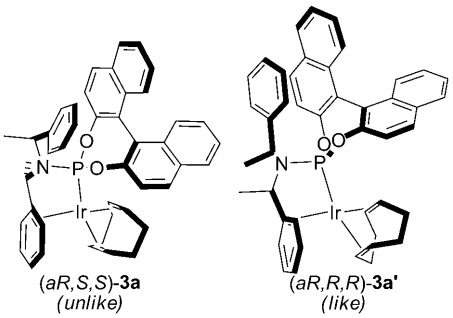

Scheme 6. Calculated structures of (*aR*,*S*,*S*)-**3a** and its putative *aR*,*R*,*R* diastereoisomer (not observed experimentally).

NMR spectroscopic studies of (*aS*,*R*,*R*)-[Ir(cod)(1,2,3,4-η-1b,κP)]$^+$ (3b): To generalize the above observations, we studied the coordination chemistry of the naphthyl-substituted P* ligand. Chloride abstraction from (*aS*,*R*,*R*)-[IrCl(cod)-(**1b**,κP)] (**2b**), which contained the 1-naphthyl-substituted

ligand (*aS*,*R*,*R*)-**1b**, gave a cationic complex, the room-temperature ^{31}P NMR spectrum of which in CD_2Cl_2 shows two singlets at $\delta = 119.8$ (major) and 111.9 ppm (minor) (5:2 ratio; Supporting Information, Figure S5). We assign these signals to diastereoisomers generated by the coordination of either enantioface of the naphthyl group. Complex **3b** is less dynamic than **3a** and the slow-exchange regime is reached at −40 °C (Supporting Information, Figure S6). Although signal overlap complicated the assignment, we were able to fully and unambiguously assign all the signals of the metal-bonded naphthyl group in both isomers by the combination of NMR spectroscopic methods described for **3a** (Scheme 7).

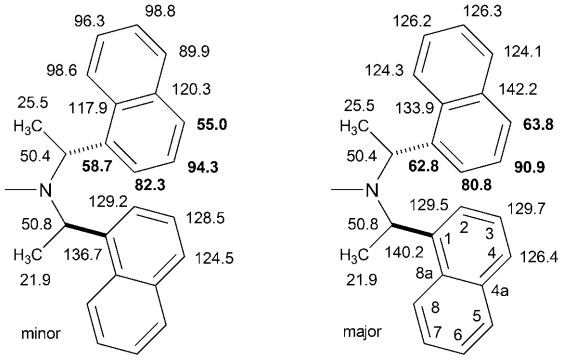

Scheme 7. ^{13}C NMR chemical shifts of the N(CH(Me)1-Np)$_2$ moiety of (*aR*,*S*,*S*)-**3b** (metal-bonded C atoms in boldface; CD_2Cl_2, 233 K). 1-Np = 1-naphthyl.

After determining the connectivity within the coordinated naphthyl ring by means of a NOESY experiment, a ^{13}C–^{1}H HMQC NMR experiment (Supporting Information, Figure S7) showed that the ^{1}H NMR signals of the H atoms in the 2, 3, and 4 positions of this ring are shifted to low frequency. Also the corresponding C atoms are significantly shielded (Scheme 7), which indicates that four instead of two C atoms are involved in the interaction with the metal (Figure S7). Therefore, we formulate this species as (*aS*,*R*,*R*)-[Ir(cod)(1,2,3,4-η-**1b**,κP)]SbF_6 (**3b**).

It should be noted that the phenethyl group of ligand **1b** binds the metal in an η^2 fashion in the previously reported [RuCl(η^6-*p*-cymene)(1,2-η-**1b**-κP)]$^+$ (**5**), which is formed as a single diastereoisomer and unambiguously features an η^2-naphthyl interaction both in solution and in the solid state, as supported by NMR and X-ray data.[8b] We conclude that the naphthyl group gives either an η^2 or η^4 interaction to achieve the 18-electron configuration of the metal, and hence its apticity is determined by the electron count of the metal.

Also, the η^4-arene–metal interaction observed in **3b** is fundamentally different—from the standpoint of orbital structure—from that previously found for the d^8 analogue [Rh(**1a**,κP)(η^6-Ph-**1a**,κP)]$^+$ (**8**),[9] in which the arene ring is bound in an η^6 fashion and acts as a four-electron donor.[20]

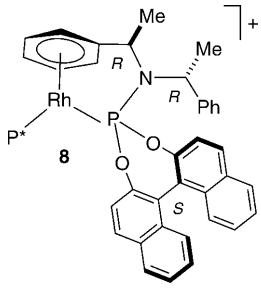

A further striking feature of **3b** is that the interconversion of its diastereoisomers is slow at room temperature, as indicated by the resolved singlets observed in the ^{31}P NMR spectrum at 25 °C, whereas most such complexes, including **3a** and **5**–**7**, are highly dynamic (the NMR signals of [RuCl(η^6-*p*-cymene)(1,2-η-Ph-P*,κP)]PF_6 are not sharp above −20 °C). We attribute this fact to an unusually high barrier to rotation of the coordinated aryl group. This may be taken as an indication that the η^4 binding mode (to give a formally five-coordinate d^8 complex) is stronger than the usually observed η^2 coordination. Additionally, naphthyl groups generally have a higher tendency to bind transition metals in an η^4 fashion than benzene rings.[21] A manifestation thereof is that the η^6/η^4 haptotropic shift ("ring slippage") is more favorable in complexes with fused polyarenes than in the benzene ones ("naphthalene effect").[21] This is because the HOMO has a lower symmetry in naphthalene (and anthracene) than benzene and features a nodal plane at the ring junction, which optimizes the d_π interaction with the nonjunction carbon atoms in the ring-slipped structure.[22] We believe that this argument qualitatively holds in the case of **3a** and **3b**, despite the fact that this comparison involves the η^2 and η^4 binding modes instead of η^6 and η^4, but a detailed orbital analysis is necessary to assess this point.

Complex **3b** has to be regarded as an 18-electron, five-coordinate complex. Therefore, we expect its structural features to deviate significantly from those of the formally square-planar **3a**. In fact, the donor set of complex **3b**, which formally consists of four C=C double bonds and one P donor, finds precedent in square-pyramidal complexes of rhodium(I) and iridium(I) in which four olefins occupy the basal positions and the P atom is apical.[23] Such a structure would imply major structural differences between the four-coordinate complex **3a** and the formally five-coordinate species **3b**. Therefore, as X-ray structural data are not yet available, we renounce to a structural analysis of **3b** in solution based on NOE contacts.

Attempted synthesis of (*aS*,*S*,*S*)-[IrCl(cod)(1b′)] (4b′): Finally, we observed a yet different pattern in the reaction of the *like* diastereoisomer of the 1-naphthyl ligand (**1b′**; Scheme 8). When $[IrCl(cod)]_2$ and (*aS*,*S*,*S*)-**1b′** (2 equiv) are dissolved in CD_2Cl_2, the ^{31}P NMR spectrum of the reaction solution recorded just after mixing shows two singlets at $\delta =$ 128.6 ppm and a second signal at $\delta = 13.2$ ppm in a 1:1 ratio, which we are unable to assign. After 10 min of reaction time, the signal at $\delta = 128.6$ ppm has disappeared, and the peak at $\delta = 13.2$ ppm is the only signal in the ^{31}P NMR spectrum. The chemical shift of $\delta = 128.6$ ppm is close to that of the cationic disubstituted complex (*aS*,*S*,*S*)-**4b′** ($\delta =$ 132.2 ppm). This suggests that the primary product is an un-

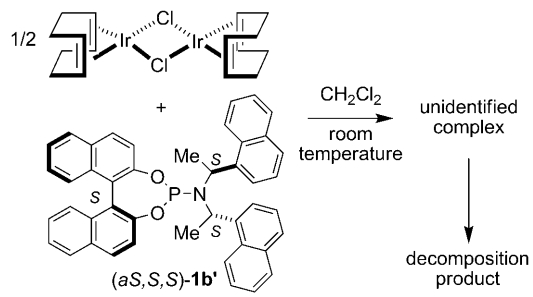

Scheme 8. Reaction of (*aS*,*S*,*S*)-**1b′** with $[IrCl(cod)]_2$ in CD_2Cl_2.

stable bis(phosphoramidite) complex that rapidly decomposes. The chemical shift of the unidentified decomposition product is suggestive of a phosphate-based structure.

Asymmetric cyclopropanation: The cationic complexes **3a**, **3b**, and **4a′** were tested in the asymmetric cyclopropanation of α-methylstyrene with ethyl diazoester (Scheme 9 and

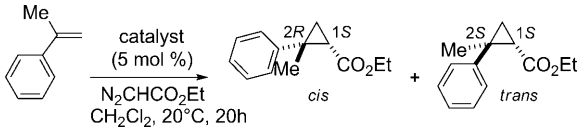

Scheme 9. Catalytic cyclopropanation of α-methylstyrene.

Table 2). In a series of preliminary experiments carried out before discovering the effects discussed above, we prepared the catalyst by chloride abstraction from the neutral species [IrCl(cod)(P*)] (P* = **1a**, **1a′**, or **1b**). The latter were prepared in situ by treating [IrCl(cod)(P*)] with the P* ligand (2 equiv versus Ir).

The results with the diastereoisomeric ligands (*aR*,*S*,*S*)-**1a** and (*aR*,*R*,*R*)-**1a′** in Table 2 show that these ligands give products with opposite absolute configuration. This intrigued us, as the X-ray studies show that the ligand conformation is controlled by the configuration of the binaphthol moiety, which is *aR* in both cases, whereas the central stereogenic element is irrelevant for the absolute configuration at iridium. However, the result is not surprising in the light of our successive finding that, under the conditions used, ligand (*aR*,*S*,*S*)-**1a** gives the cationic monosubstituted complex (*aR*,*S*,*S*)-[Ir(cod)(1,2-η-**1a**,κP)]$^+$ (**3a**), which is the actual catalyst in run 1 (Table 2). In contrast, the diastereoisomeric ligand (*aR*,*R*,*R*)-**1a′** yields, all other things being equal, the cationic disubstituted species [Ir(cod){(R_a,*R*,*R*)-**1a′**,κP}$_2$]$^+$ (**4a′**, 0.5 equiv; along with unidentified non-phosphoramidite-containing complexes, see below). Therefore, as different complexes are formed in solution under the conditions of run 3 (Table 2) instead of a monosubstituted P* complex, no prediction concerning the sense of induction is possible, in fact, as the structures of the catalysts containing **1a** and **1a′** are entirely different.

Under the conditions used in run 3, the ligand scrambling reaction depicted in Scheme 4 produces **4a′** along with an equivalent amount of non-phosphoramidite-containing complexes. However, it should be noted that use of the correct amount of the P* ligand, that is, a 2:1 ratio to iridium(I), in the reaction with the *like* ligand (*aR*,*R*,*R*)-**1a′** (run 4, Table 2) did not change significantly the outcome of the reaction with respect to run 3. Interestingly, the similarity between the reaction results of runs 3 and 4 indicates that the latter species are not—or only weakly—catalytically active in cyclopropanation. As this is not a general rule, and other reactions may well behave differently, this shows again that the use of P*-containing catalysts prepared in situ without further characterization is potentially misleading.

A further feature that confused us at first is that (*aR*,*S*,*S*)-**1a** and (*aS*,*R*,*R*)-**1b** give cyclopropanes with the same absolute configuration (runs 1 and 6, Table 2) despite ligands **1a** and **1b** have opposite absolute configurations. Again, this can be rationalized by assuming that the η^2 or η^4 interactions formed by these ligands have different influences on the stereochemical course of the catalytic reaction. Admittedly, this is speculative, but not arbitrary in view of the significant differences between the 16-electron, square-planar **3a** and **3b**, which is formally a five-coordinate, 18-electron species. An interesting observation is that the enantioselectivity with **1a** and **1b**, which act as chelating ligands in **3a** and **3b**, is strongly enhanced at low temperature (runs 2 and 7, Table 2), but not with **1a′**, which gives the disubstituted complex **4a′** (run 5). This is a further indication that the weak secondary π-arene–metal interaction plays a pivotal role.

Obviously, these results are interesting as an example of apparently random stereochemical behavior that can be rationalized by an accurate analysis of the complexes actually present in solution under catalytic conditions, rather than for their relevance in terms of catalyst performance. However, to the best of our knowledge, this is the first example of iridium(I)-catalyzed cyclopropanation, the closest analogues being *N*,*N*′-bis(salicylidene) ethylenediamine (salen)-based iridium(III) catalysts[24] and

Table 2. Cyclopropanation of α-methylstyrene.[a]

Run	P* ligand	Equiv P*[b]	Conv.[c]	Yield [%]	*cis*/*trans*	*ee* (*cis*) [%][d]	*ee* (*trans*) [%][d]
1	(*aR*,*S*,*S*)-**1a**	2	39	12	55:45	54 (1*S*,2*R*)	35 (1*S*,2*S*)
2[c]	(*aR*,*S*,*S*)-**1a**	2	12	5	78:22	85 (1*S*,2*R*)	55 (1*S*,2*S*)
3	(*aR*,*R*,*R*)-**1a′**	2	92	2	89:11	9 (1*R*,2*S*)	36 (1*R*,2*R*)
4	(*aR*,*R*,*R*)-**1a′**	4	85	10	85:15	12 (1*R*,2*S*)	39 (1*R*,2*R*)
5[c]	(*aR*,*R*,*R*)-**1a′**	4	34	2	89:11	14 (1*R*,2*S*)	39 (1*R*,2*R*)
6	(*aS*,*R*,*R*)-**1b**	2	39	31	83:17	4 (1*S*,2*R*)	21 (1*S*,2*S*)
7[c]	(*aS*,*R*,*R*)-**1b**	2	15	7	89:11	85 (1*S*,2*R*)	81 (1*S*,2*S*)

[a] Reaction conditions: ethyl diazoacetate (480 μmol) in CH_2Cl_2 was added over 6 h to a CH_2Cl_2 solution of styrene (480 μmol) and the catalyst (24 μmol, 5 mol%) at room temperature. The total reaction time was 20 h. [b] Equivalents of ligand (see Experimental Section). [c] At −30 °C. [d] *ee* = enantiomeric excess.

some achiral rhodium(I) species that generally display low or no activity at room temperature.[25,26] Finally, although no mechanistic hypothesis would be reasonable to date, catalytic cyclopropanation with square-planar d^8 complexes is potentially interesting from a mechanistic viewpoint because it might involve a metallacyclic intermediate rather than nucleophilic attack of the olefin on a metal carbene complex, as generally assumed with transition metals that are not prone to oxidative addition.[27]

Overall relevance to catalysis: We have shown that subtle changes in the relative configuration of the stereogenic elements of phosphoramidite ligands bearing benzylic appendages at the nitrogen atom dramatically affect their coordination chemistry. Thus, the widely differing catalytic behavior shown by the diastereoisomeric ligands (*aR*,*S*,*S*)-**1a** (*unlike*) and (*aR*,*R*,*R*)-**1a′** (*like*) in iridium(I)-catalyzed cyclopropanation correlate with the different coordination behavior of the P* ligands.

We also suggest that our observations might be relevant to other catalysts that show apparently random stereochemical outcomes, such as in the iridium(I)-catalyzed asymmetric allylic alkylation of monosubstituted allylic acetates.[6] The reactions with the diastereoisomeric ligands (*aR*,*S*,*S*)-**1a** (*unlike*) and (*aS*,*S*,*S*)-**1a′** (*like*) showed widely different stereochemical courses without apparent pattern. Although chloride abstraction has not been taken into consideration with this catalytic system,[16a] this possibility cannot be ruled out for iridium(I) complexes in THF and in the presence of sodium malonate, the Na^+ counterion of which may well act as a chloride scavenger. Therefore, the formation of complexes with different composition (that is, either mono- or bis(P*)-substituted) according to the relative configuration of P* is a possibility that deserves consideration.

Furthermore, Hayashi et al. recently reported an asymmetric [5+2] cycloaddition of alkyne-vinylcyclopropanes catalyzed by cationic rhodium(I) complexes, in which the best-performing ligands are (*aS*,*R*,*R*)-**1a** and (*aS*,*S*,*S*)-**1a**.[7] Again, largely different behaviors are observed for the *like* (31% yield, 75% *ee*) and *unlike* (88% yield, 99% *ee*) diastereoisomers of the P* ligand. The proposed mechanistic interpretation is based on the involvement of an η^2-arene complex, the structure of which is derived by analogy with the previously reported (*aR*,*S*,*S*)-[Rh(nbd)(1,2-η-Ph-**1a**,κP)]$^+$ (**6**).[9] Although the present results for iridium(I) cannot be extrapolated to rhodium(I), the lower activity observed with the *like* ligand (*aS*,*S*,*S*)-**1a** may well be explained by the formation of a bis(phosphoramidite) complex. Clearly, it would not be surprising that a disubstituted complex was less reactive than the mono-P* complex with an η^2 interaction formed by the *unlike* diastereoisomer.

In this context, it should be also mentioned that, beyond furnishing a handle to fine-tune the structure, stereochemistry, and reactivity of P*-containing complexes, our findings contribute to a deeper understanding of the subtle steric effects that involve phosphoramidite ligands. This is also highly desirable in view of the wide application of phosphoramidite ligands in combinatorial transition-metal catalysis,[1d] in which subtle energy differences between similar structures play a pivotal role. Therefore, it is of the utmost importance to be aware of and take into account any conceivable coordination mode of the P* ligands.

Conclusion

The present results show that the coordination behavior of P* ligands bearing dangling arenes is still largely unpredictable to date. Therefore, assumptions concerning the structure and formulation of catalysts prepared in situ by treating suitable metal-containing precursors with phosphoramidite ligands should be supported by adequate characterization of the species actually formed in solution.

Experimental Section

General: Reactions with air- or moisture-sensitive materials were carried out under an argon atmosphere using Schlenk techniques, or in a glove box under purified nitrogen. (*S*)-(−)-Bis(1-phenylethyl)amine hydrochloride was obtained from Aldrich. (*R*)-(−)-1,1′-Bi-2-naphthol (binol) and phosphorus trichloride were purchased from Fluka. PCl_3 was distilled immediately before use. All other commercially available reagents were used without further purification. Solvents were purified by standard procedures: CH_2Cl_2 and CD_2Cl_2 were distilled from CaH_2. $[RhCl(cod)]_2$ and $[IrCl(cod)]_2$ were prepared according to literature procedures.[28] Mass spectra were measured by the MS service (Laboratorium für Organische Chemie, ETH Zürich). The high-resolution (HR) MALDI spectra were recorded on an IonSpec Ultima HR MALDI-FT-ion cyclotron resonance mass spectrometer at 4.7 T with a *trans*-2-[3-(4-*tert*-butylphenyl)-2-methyl-2-propylidene]-malononitrile (DCTB) matrix. Elemental analyses were carried out by the Laboratory of Microelemental Analysis (Laboratorium für Organische Chemie, ETH Zürich). ^{1}H (700, 500, and 300 MHz), ^{31}P (283, 202, and 121 MHz), and ^{13}C (176, 126, 100, and 76 MHz) NMR spectra were recorded on Bruker Avance 700, 500, 400, and 300 MHz spectrometers, respectively, as CD_2Cl_2 solutions, unless otherwise stated. Chemical shifts δ are quoted in parts per million (ppm) relative to tetramethylsilane. ^{31}P NMR chemical shifts were referenced externally to 85% H_3PO_4 ($\delta = 0.0$ ppm). Coupling constants J are given in Hertz. A chemical-shift range is specified for multiplets broader than 0.1 ppm, whereas multiplets < 0.1 ppm are identified by the chemical shift of their center. The activation energy (E_a) for the rotation of the η^2-bound phenyl ring in the cationic Ir^I complex **3a** was calculated by the Arrhenius equation $k(T) = e^{-E_a/RT}$. The values for $k(T)$ were determined by line-shape analysis of the ^{1}H NMR spectra between −80 and −10 °C with the program MEXICO.[29]

(*aR*,*S*,*S*)-[IrCl(cod)(1a,κP)] (2a): $[IrCl(cod)]_2$ (201.5 mg, 0.3 mmol) and ligand (*aR*,*S*,*S*)-**1a** (323.8 mg, 0.6 mmol) were dissolved in CH_2Cl_2 (2 mL) and the resulting orange solution was stirred for 30 min at room temperature. After evaporating the solvent, the crude product was washed with diethyl ether and pentane. Bright orange platelets crystallized from diethyl ether within two days and were washed with CH_2Cl_2 and dried in a vacuum. The crystals contained one CH_2Cl_2 unit per complex molecule, as shown by ^{1}H NMR spectroscopy. Yield: 287.7 mg, 55%; ^{1}H NMR (300 MHz, $CDCl_3$): $\delta = 1.05$ (m, 1H; cod C*H*H′), 1.51 (m, 1H; cod C*H*H′), 1.63 (d, $^3J_{H,H} = 5.3$ Hz, 6H; NCHC*H*$_3$), 1.74–2.0 (m, 5H; cod C*H*H′), 2.17 (m, 1H; cod C*H*H′), 2.65 (m, 1H; cod C*H*=CH), 3.38 (dq, $^3J_{H,H} = 10.5$, 5.2 Hz, 2H; NC*H*CH$_3$), 3.76 (m, 1H; cod C*H*=CH), 5.59 (m, 1H; cod C*H*=CH), 5.79 (m, 1H; cod C*H*=CH), 6.97 (d, $^3J_{H,H} = 2.0$ Hz, 1H; arom H), 6.98–7.12 (m, 11H; arom H), 7.17–7.27 (m, 5H; arom H), 7.46 (d, $^3J_{H,H} = 6.5$ Hz, 1H; arom H), 7.65 (d, $^3J_{H,H} = 5.6$ Hz, 1H; arom H),

7.78 (d, $^3J_{H,H}$=8.1 Hz, 1H; arom H), 8.87 (d, $^3J_{H,H}$=8.9 Hz, 1H; arom H), 8.7 ppm (d, $^3J_{H,H}$=8.8 Hz, 1H; arom H); ^{13}C NMR (100 MHz, $CDCl_3$): δ=19.5 (d, $^3J_{P,C}$=5.2 Hz, NCH*C*H$_3$), 20.3 (d, $^3J_{P,C}$=5.1 Hz, NCH*C*H$_3$), 28.96 (d, $^2J_{P,C}$=1.6 Hz, *C*H$_2$CH=CH), 29.2 (d, $^3J_{P,C}$=2.1 Hz, *C*H$_2$CH=CH), 32.7 (d, $^2J_{P,C}$=1.9 Hz, *C*H$_2$CH=CH), 34.7 (d, $^2J_{P,C}$=2.0 Hz, *C*H$_2$CH=CH), 50.3 (d, $^2J_{P,C}$=12.3 Hz, N*C*HCH$_3$), 52.6 (d, $^2J_{P,C}$=13.1 Hz, N*C*HCH$_3$), 97.2 (d, $^2J_{P,C}$=18.2 Hz, CH$_2$*C*H=CH), 98.5 (d, $^2J_{P,C}$=18.0 Hz, CH$_2$*C*H=CH), 102.2 (d, $^2J_{P,C}$=18.6 Hz, CH$_2$*C*H=CH), 103.4 (d, $^2J_{P,C}$=19.0 Hz, CH$_2$*C*H=CH), 121.2 (binol), 121.6 (binol), 124.1 (binol), 125.3 (binol), 125.8 (binol), 126.2 (binol), 126.2 (binol), 126.7 (binol), 127.3 (2C, *meta* C, Ph), 127.4 (binol), 127.8 (2C, *meta* C, Ph), 127.97 (2C, *ortho* C, Ph), 128.2 (2C, *meta* C, Ph), 128.6 (*para* C, Ph), 128.8 (binol), 130.2 (binol), 130.6 (*para* C, Ph), 131.4 (binol), 132.3 (binol), 132.7 (binol), 133.0 (binol), 133.3 (binol), 138.2 (*ipso* C, Ph), 138.8 (*ipso* C, Ph), 144.5 (binol), 149.5 (binol), 150.7 (binol), 150.8 ppm (binol); ^{31}P{^{1}H} NMR (121 MHz, $CDCl_3$): δ=114.9 ppm (s); HRMS (MALDI): *m*/*z*: calcd for $C_{44}H_{40}NO_2PIr$: 838.2423; found: 838.2427 $[M-ClH_2]^+$; elemental analysis (%) calcd for $C_{45}H_{42}ClIrNO_2P$: C 60.37, H 4.84, N 1.6; found: C 60.09, H 4.9, N 1.81.

(*aR*,*R*,*R*)-[IrCl(cod)(1a′,κP)] (2a′): Complex **2a′** was prepared from $[IrCl(cod)]_2$ and (*aR*,*R*,*R*)-**1a′** as described above for **2a**. Yield: 288.9 mg, 55%; ^{1}H NMR (300 MHz, $CDCl_3$): δ=1.03 (s, 2H; cod C*H*H′), 1.14–1.57 (m, 5H; cod CH*H*′), 1.71 (d, $^3J_{H,H}$=7.1 Hz, 6H; NCHC*H*$_3$), 2.25 (m, 1H; cod C*H*H′), 2.44 (m, 1H; cod C*H*=CH), 3.24 (m, 2H; NC*H*CH$_3$), 4.46 (m, 1H; cod C*H*=CH), 5.31 (m, 1H; cod C*H*=CH), 5.48 (m, 1H; cod C*H*=CH), 6.82 (d, $^3J_{H,H}$=8.8 Hz, 1H; arom H), 7.08–7.32 (m, 16H; arom H), 7.35 (d, $^3J_{H,H}$=8.4 Hz, 1H; arom H), 7.92 (d, $^3J_{H,H}$=8.9 Hz, 1H; arom H), 7.98 (d, $^3J_{H,H}$=8.2 Hz, 1H; arom H), 8.03 (d, $^3J_{H,H}$=8.2 Hz, 1H; arom H), 8.13 ppm (s, 1H; arom H); ^{13}C NMR (100 MHz, $CDCl_3$): δ=21.2 (d, $^3J_{P,C}$=5.0 Hz, NCH*C*H$_3$), 22.0 (d, $^3J_{P,C}$=5.1 Hz, NCH*C*H$_3$), 28.13 (d, $^2J_{P,C}$=3.3 Hz, cod *C*H$_2$CH=CH), 29.36 (d, $^2J_{P,C}$=2.6 Hz, cod *C*H$_2$CH=CH), 32.84 (d, $^3J_{P,C}$=3.5 Hz, cod *C*H$_2$CH=CH), 33.4 (d, $^3J_{P,C}$=3.4 Hz, cod *C*H$_2$CH=CH), 55.0 (d, $^2J_{P,C}$=8.7 Hz, N*C*HCH$_3$), 57.2 (d, $^2J_{P,C}$=8.7 Hz, N*C*HCH$_3$), 89.3 (cod CH$_2$*C*H=CH), 90.1 (cod CH$_2$*C*H=CH), 102.15 (d, $^2J_{P,C}$=14.7 Hz, cod CH$_2$*C*H=CH), 101.4 (d, $^2J_{P,C}$=17.0 Hz, cod CH$_2$*C*H=CH), 121.3 (binol), 121.7 (binol), 123.4 (binol), 125.0 (binol), 125.3 (binol), 125.9 (2C, *meta* C, Ph), 126.2 (binol), 126.7 (2C, *ortho* C, Ph), 126.9 (binol), 127.0 (binol), 127.4 (2C, *meta* C, Ph), 127.7 (2C, *ortho* C, Ph), 127.8 (binol), 127.98 (binol), 128.1 (*para* C, Ph), 128.3 (binol), 128.5 (binol), 128.6 (binol), 128.9 (*para* C, Ph), 129.6 (binol), 129.9 (binol), 130.8 (binol), 131.7 (binol), 132.3 (binol), 132.7 (binol), 141.9 (binol), 142.4 (*ipso* C, Ph), 142.9 (*ipso* C, Ph), 145.3 (binol), 148.7 ppm (binol); ^{31}P{^{1}H} NMR (121 MHz, $CDCl_3$): δ=114.5 ppm (s); HRMS (MALDI): *m*/*z*: calcd for $C_{44}H_{40}NO_2PIr$: 838.2423; found: 838.2420 $[M-ClH_2]^+$; elemental analysis calcd for $C_{44}H_{42}ClIrNO_2P$: C 60.37, H 4.84, N 1.6; found: C 60.31, H 4.85, N 1.62.

(*aS*,*R*,*R*)-[IrCl(cod)(1b-κP)] (2b): Complex **2b** was prepared from $[IrCl(cod)]_2$ and (*aS*,*R*,*R*)-**1b** as described above for **2a**. Yield: 156.3 mg, 89%; ^{1}H NMR (300 MHz, $CDCl_3$): δ=1.26 (d, $^3J_{H,H}$=7.2 Hz, 6H; NCHC*H*$_3$), 2.02 (s, 2H; cod C*H*H′), 2.28 (m, 5H; cod CH*H*′), 2.91 (m, 1H; cod C*H*H′), 3.11 (m, 1H; cod C*H*=CH), 4.06 (m, 2H; NC*H*CH$_3$), 4.27 (m, 1H; cod C*H*=CH), 5.20 (m, 1H; cod C*H*=CH), 5.36 (m, 1H; cod C*H*=CH), 7.16 (d, $^3J_{H,H}$=8.3 Hz, 4H; arom H), 7.25–7.56 (m, 14H; arom H), 7.95 ppm (d, $^3J_{H,H}$=7.8 Hz, 4H; arom H); ^{13}C NMR (100 MHz, $CDCl_3$): δ=15.1(NCH*C*H$_3$), 19.97 (NCH*C*H$_3$), 26.1 (cod *C*H$_2$CH=CH), 27.2 (cod *C*H$_2$CH=CH), 31.5 (cod *C*H$_2$CH=CH), 32.1 (cod *C*H$_2$CH=CH), 48.0 (N*C*HCH$_3$), 51.7 (d, $^2J_{P,C}$=8.7 Hz, N*C*HCH$_3$), 58.4 (cod CH$_2$*C*H=CH), 59.7 (cod CH$_2$*C*H=CH), 63.3 (cod CH$_2$*C*H=CH), 67.8 (cod CH$_2$*C*H=CH), 98.3 (d, $^2J_{P,C}$=4.1 Hz, arom), 111.1 (arom), 123.15 (arom), 123.27 (d, $J_{P,C}$=3.4 Hz, arom), 123.4 (arom), 123.5 (d, $J_{P,C}$=2.3 Hz, arom), 123.6 (arom), 124.6 (d, $J_{P,C}$=3.1 Hz, arom), 125.40 (arom), 125.7 (arom), 126.1 (arom), 126.8 (d, $J_{P,C}$=7.0 Hz, arom), 127.3 (arom), 127.4 (arom), 127.6 (arom), 127.7 (arom), 127.8 (arom), 128.0 (arom), 128.2 (arom), 128.4 (d, $J_{P,C}$=7.1 Hz, arom), 128.6 (arom), 129.3 (arom), 130.1 (arom), 131.7 (d, $J_{P,C}$=1.2 Hz, arom), 136.99 (arom), 137.7 (arom), 142.0 (arom), 142.7 (arom), 148.06 (d, $J_{P,C}$=5.7 Hz, arom), 149.0 ppm (arom); ^{31}P{^{1}H} NMR (121 MHz, $CDCl_3$): δ=122.8 ppm (s); HRMS (MALDI): *m*/*z*: calcd for $C_{52}H_{46}NO_2PIr$: 940.2894; found: 940.2884 $[M-Cl]^+$; elemental analysis calcd for $C_{52}H_{46}ClIrNO_2P$: C 64.02, H 4.75, N 1.44;. found: C 64.05, H 4.89, N 1.32.

(*aS*,*S*,*S*)-[IrCl(cod)(1b′-κP)] (2b′): Complex **2b′** was prepared from $[IrCl(cod)]_2$ and (*aS*,*S*,*S*)-**1b′** as described above for **2a**. Yield: 145.8 mg, 83%; ^{1}H NMR (300 MHz, $CDCl_3$): δ=1.18 (d, $^3J_{H,H}$=8.0 Hz, 6H; NCHC*H*$_3$), 2.02 (s, 2H; cod C*H*H′), 2.21–2.39 (m, 5H; cod CH*H*′), 2.98 (m, 1H; cod C*H*H′), 3.2 (m, 1H; cod C*H*=CH), 4.00–4.2 (m, 2H; NC*H*CH$_3$), 4.3 (m, 1H; cod C*H*=CH), 5.2 (m, 1H; cod C*H*=CH), 5.4 (m, 1H; cod C*H*=CH), 7.2 (d, $^3J_{H,H}$=8.3 Hz, 2H; arom H), 7.3–7.5 (m, 14H; arom H), 7.95 (d, $^3J_{H,H}$=7.8 Hz, 4H; arom H), 8.02 ppm (d, $^3J_{H,H}$=8.9 Hz, 2H; arom H); ^{13}C NMR (100 MHz, $CDCl_3$): δ=10.9 (NCH*C*H$_3$), 24.2 (NCH*C*H$_3$), 31.8 (cod *C*H$_2$HC=CH), 33.0 (cod *C*H$_2$HC=CH), 34.1 (cod *C*H$_2$HC=CH), 35.3 (cod *C*H$_2$HC=CH), 50.4 (d, $^2J_{P,C}$=8.7 Hz, N*C*HCH$_3$), 62.1 (N*C*HCH$_3$), 88.1 (cod CH$_2$*C*H=CH), 89.2 (cod CH$_2$*C*H=CH), 97.6 (cod CH$_2$*C*H=CH), 98.9 (cod CH$_2$*C*H=CH), 111.2 (d, $^2J_{P,C}$=5.2 Hz, arom), 117.8 (arom), 124.0 (d, $J_{P,C}$=11.8 Hz, arom), 125.8 (arom), 125.9 (arom), 126.5 (arom), 126.8 (arom), 127.0 (arom), 127.2 (arom), 127.3 (arom), 127.5 (arom), 127.6 (arom), 127.7 (arom), 128.4 (arom), 129.5 (arom), 131.3 (arom), 133.6 (arom), 136.5 (arom), 138.8 (arom), 140.2 (arom), 147.3 (arom), 148.2 (arom), 148.9 (arom), 149.1 (arom), 152.8 (arom), 162.3 ppm (arom); ^{31}P{^{1}H} NMR (121 MHz, $CDCl_3$): δ=120.5 ppm (s); HRMS (MALDI): *m*/*z*: calcd for $C_{52}H_{46}NO_2PIr$ 940.2894, found 940.2884 $[M-Cl]^+$; elemental analysis calcd for $C_{52}H_{46}ClIrNO_2P$: C 64.02, H 4.75, N 1.44; found: C 63.95, H 4.72, N 1.43.

(*aR*,*S*,*S*)-[Ir(cod)(1,2-η-1a,κP)]SbF$_6$ (3a): $[IrCl(cod)]_2$ (100.0 mg, 0.15 mmol) and ligand (R_a,S_C,S_C)-**1a** (160.6 mg, 0.3 mmol) were dissolved in CH_2Cl_2 (1 mL), and the resulting bright orange solution was stirred at room temperature during 30 min. Then, $AgSbF_6$ (102.3 mg, 0.3 mmol) was added, and the resulting red mixture was stirred vigorously for 2 h. After filtration and evaporation of the solvent, the crude product was washed with diethyl ether and pentane, and the resulting red powder was dried in a vacuum. The crystals contained one CH_2Cl_2 unit per complex molecule, as shown by ^{1}H NMR spectroscopy. Yield: 245.6 mg, 74%; ^{1}H NMR (700 MHz, CD_2Cl_2, −80°C): δ=1.2 (m, 1H; cod C*H*H′), 1.3 (m, 1H; cod C*H*H′), 1.4 (m, 1H; cod C*H*H′), 1.56 (m, 1H; cod CH*H*′), 1.57 (m, 3H; free NCHC*H*$_3$), 1.58 (m, 1H; cod C*H*H′), 1.74 (m, 1H; cod CH*H*′), 1.86 (d, $^3J_{P,H}$=8.1 Hz, 1H; cod C*H*=CH *trans* to P+1H; cod C*H*=CH), 2.13 (m, 3H; coord. NCHC*H*$_3$), 2.16 (m, 1H; cod C*H*H′), 2.27 (m, 1H; cod C*H*H′), 4.15 (m, 1H; cod C*H*=CH), 4.12 (m, 1H; coord. NC*H*CH$_3$), 4.63 (m, 1H; free NC*H*CH$_3$), 5.55 (d, $^3J_{P,H}$=10.2 Hz, 1H; cod C*H*=CH *trans* to P), 6.57 (s, 1H; C^2*H*, coord. Ph), 7.08 (t, $^3J_{H,H}$=7.21 Hz, 1H; C^4*H*, coord. Ph), 7.17 (t, $^3J_{H,H}$=7.0 Hz, 1H; *para* C*H*, free Ph), 7.25 (t, $^3J_{H,H}$=7.2 Hz, 2H; *meta* C*H*, free Ph), 7.42 (t, $^3J_{H,H}$=7.0 Hz, 2H; *ortho* C*H*, free Ph), 7.52 (s, 1H; C^6*H*, coord. Ph), 7.53–7.67 (m, 8H; binol H), 7.72 (t, $^3J_{H,H}$=7.0 Hz, 1H; C^5*H*, coord. Ph), 8.07 (t, $^3J_{H,H}$=8.3 Hz, 1H; C^3*H*, coord. Ph), 8.08 (d, $^3J_{H,H}$=8.3 Hz, 1H; binol H), 8.15 (d, $^3J_{H,H}$=8.8 Hz, 1H; binol H), 8.19 (d, $^3J_{H,H}$=8.9 Hz, 1H; binol H), 8.27 ppm (d, $^3J_{H,H}$=8.9 Hz, 1H; binol H); ^{13}C NMR (176 MHz, CD_2Cl_2, −80°C): δ=20.1 (free NCH*C*H$_3$), 23.9 (cod *C*H$_2$CH=CH), 24.3 (d, $^2J_{P,C}$=3.5 Hz, coord. NCH*C*H$_3$), 30.7 (cod *C*H$_2$CH=CH), 31.3 (cod *C*H$_2$CH=CH), 35.7 (cod *C*H$_2$CH=CH), 48.8 (d, $^2J_{P,C}$=27.4 Hz, coord. N*C*HCH$_3$), 49.4 (d, $^2J_{P,C}$=27.1 Hz, free N*C*HCH$_3$), 60.7 (cod CH$_2$*C*H=CH), 68.2 (cod CH$_2$*C*H=CH), 96.2 (C^2, coord. Ph), 108.7 (d, $^2J_{P,C}$=6.8 Hz, cod CH$_2$*C*H=CH *trans* to P), 111.3 ($^2J_{P,C}$=13.4 Hz, cod CH$_2$*C*H=CH *trans* to P), 121.5 (binol), 122.1 (binol), 122.3 (binol), 126.1 (binol), 126.3 (binol), 126.8 (binol), 127.0 (binol), 127.1 (binol), 127.2 (binol), 127.9 (binol), 128.2 (3C, C^6, coord. Ph+*ortho* C, free Ph), 128.5 (2C, C^4, coord. Ph+*para* C, free Ph), 128.8 (binol), 129.0 (2C, *meta* C of free Ph), 131.4 (binol), 131.42 (binol), 131.5 (binol), 131.8 (binol), 132.0 (binol), 132.3 (binol), 135.0 (C^5, coord. Ph), 138.6 (*ipso* C of free Ph), 140.5 (C^1, coord. Ph), 142.7 (C^3, coord. Ph), 147.0 (binol), 147.1 (binol), 147.3 ppm (binol). Additionally, the ^{13}C NMR signals of the bis(1-phenylethyl)amino moiety are summarized in Scheme 3; ^{31}P{^{1}H} NMR (283 MHz, CD_2Cl_2): δ=118.4 ppm (s); HRMS (MALDI): *m*/*z*: calcd for $C_{44}H_{42}NO_2PIr$: 838.2423; found: 838.2417 $[M-SbF_6]^+$; elemental analysis calcd for $C_{45}H_{44}NCl_2IrO_2P$: C 46.57, H 3.82, N 1.30; found: C 46.39, H 3.94, N 1.21.

(*aS*,*R*,*R*)-[Ir(cod)(1,2,3,4-η-1b,κP)]SbF$_6$ (3b): Complex **3b** was prepared as described for **3a**. Yield: 83% (224.4 mg); elemental analysis calcd for $C_{52}H_{46}IrNO_2PSbF_6$: C 53.12, H 3.94, N 1.19; Found: C 53.3, H 3.63, N 1.16; HRMS (MALDI): *m*/*z*: calcd for $C_{52}H_{46}NO_2PIrSbF_6$: 940.1207; found: 940.2894 $[M-SbF_6]^+$. The ^{31}P NMR data indicated that **3b** exists as two isomers in a 5:2 ratio, attributed to the generation of diastereoisomers upon coordination of either enantioface of the 1-naphthyl (Np) group. Major isomer: ^{1}H NMR (700 MHz, $CDCl_3$, −40 °C): δ = 1.22 (m, 1H; cod C*H*H′), 1.34 (m, 1H; cod C*H*H′), 1.48 (d, $^3J_{H,H}$ = 6.9 Hz, 3H; NCHC*H*$_3$, free Np), 1.55 (m, 1H; cod C*H*H′), 1.68 (d, $^3J_{H,H}$ = 5.7 Hz, 3H; NCHC*H*$_3$, coord. Np), 2.01 (m, 1H; cod C*H*H′), 2.29 (m, 1H; cod C*H*H′), 2.51 (m, 1H; cod C*H*H′), 2.81 (m, 1H; cod C*H*H′), 3.24 (m, 1H; cod C*H*H′), 4.16 (d, $^3J_{H,H}$ = 8.1 Hz, 1H; cod C*H*=CH), 4.27 (m, 1H; cod C*H*=CH *trans* to P), 4.50 (m, 1H; NC*H*CH$_3$, coord. Np), 4.80 (m, 1H; C^4*H*, coord. Np), 4.91 (m, 1H; NC*H*CH$_3$, free Np), 4.96 (m, 1H; cod C*H*=CH *trans* to P), 5.29 (m, 1H; cod C*H*=CH), 5.64 (s, 1H; C^2*H*, coord. Np), 6.34 (d, $^3J_{H,H}$ = 5.8 Hz, 1H; C^3*H*, coord. Np), 7.03 (t, $^3J_{H,H}$ = 6.0 Hz, 1H; C^6*H*, coord. Np), 7.04 (m, 1H; C^8*H*, coord. Np), 7.07 (t, $^3J_{H,H}$ = 5.9 Hz, 1H; C^7*H*, coord. Np), 7.29 (d, $^3J_{H,H}$ = 5.8 Hz, 1H; C^5*H*, coord. Np), 7.06 (d, $^3J_{H,H}$ = 7.1 Hz, 1H; binol H), 7.22 (m, 1H; binol H), 7.24 (d, $^3J_{H,H}$ = 7.2 Hz, 1H; binol H), 7.40 (m, 1H; binol H), 7.41 (m, 1H; binol H), 7.52 (m, 1H; binol H), 7.56 (d, $^3J_{H,H}$ = 3.6 Hz, 1H; free Np C^3*H*), 7.58 (m, 1H; binol H), 7.62 (m, 1H; binol H), 7.67 (m, 1H; binol H), 7.72 (d, $^3J_{H,H}$ = 8.2 Hz, 1H; C^4*H*, free Np), 7.75 (m, 1H; C^8*H*, free Np), 7.76 (m, 1H; C^6*H*, free Np), 8.06 (d, $^3J_{H,H}$ = 8.2 Hz, 1H; binol H), 8.09 (m, 1H; C^7*H*, free Np), 8.11 (d, $^3J_{H,H}$ = 8.9 Hz, 1H; binol H), 8.17 (d, $^3J_{H,H}$ = 8.3 Hz, 1H; binol H), 8.23 (d, $^3J_{H,H}$ = 9.0 Hz, 1H; C^2*H*, free Np), 8.39 ppm (m, 1H; C^5*H*, free Np); ^{13}C NMR (176 MHz, $CDCl_3$, −40 °C): δ = 23.8 (free NCH*C*H$_3$), 25.3 (cod *C*H$_2$CH=CH), 26.1 (coord. NCH*C*H$_3$), 27.5 (cod *C*H$_2$CH=CH), 33.0 (cod *C*H$_2$CH=CH), 36.4 (cod *C*H$_2$CH=CH), 50.1 (d, $^2J_{P,C}$ = 21.9 Hz, free N*C*HCH$_3$), 52.6 (d, $^2J_{P,C}$ = 23.2 Hz, coord. N*C*HCH$_3$), 62.8 (C^1, coord. Np), 63.8 (C^4, coord. Np), 80.8 (C^2, coord. Np), 84.3 (cod CH$_2$*C*H=CH), 85.7 (cod CH$_2$*C*H=CH), 87.9 (cod CH$_2$*C*H=CH), 89.1 (binol), 89.5 (binol), 90.9 (C^3, coord. Np), 98.7 (cod CH$_2$*C*H=CH), 98.6 (binol), 98.8 (binol), 102.2 (binol), 120.5 (binol), 120.6 (binol), 120.7 (binol), 121.5 (binol), 121.6 (binol), 121.7 (binol), 122.5 (binol), 124.1 (C^5, coord. Np), 124.3 (C^8, coord. Np), 125.5 (binol), 126.2 (C^7, coord. Np), 126.3 (C^6, coord. Np), 126.4 (C^4, free Np), 126.9 (C^8, free Np), 127.2 (C^5, free Np), 127.3 (C^6, free Np), 127.5 (C^7, free Np), 127.8 (binol), 128.3 (binol), 128.8 (binol), 129.0 (binol), 129.2 (binol), 129.5 (C^2, free Np), 129.7 (C^3, free Np), 132.7 (C^{4a}, free Np), 133.7 (C^{8a}, free Np), 133.9 (C^{8a}, coord. Np), 140.2 (C^1, free Np), 142.2 (C^{4a}, coord. Np), 147.3 (binol), 148.9 ppm (binol); ^{31}P{^{1}H} NMR (121 Hz, $CDCl_3$): δ = 119.8 ppm (s); minor isomer: ^{1}H NMR (700 MHz, $CDCl_3$, −40 °C): δ = 1.20 (m, 1H; cod C*H*H′), 1.28 (m, 1H; cod C*H*H′), 1.36 (d, $^3J_{H,H}$ = 6.5 Hz, 3H; NCHC*H*$_3$ of free Np), 1.56 (m, 1H; cod C*H*H′), 1.68 (d, $^3J_{H,H}$ = 5.2 Hz, 3H; NCHC*H*$_3$, coord. Np), 2.04 (m, 1H; cod C*H*H′), 2.37 (m, 1H; cod C*H*H′), 2.54 (m, 1H; cod C*H*H′), 2.76 (m, 1H; cod C*H*H′), 3.33 (m, 1H; cod C*H*H′), 4.30 (m, 1H; NC*H*CH$_3$, coord. Np), 4.40 (d, $^3J_{H,H}$ = 8.1 Hz, 1H; cod C*H*=CH *trans* to P), 4.67 (m, 1H; cod C*H*=CH), 4.71 (m, 1H; C^4*H*, coord. Np), 5.07 (br. s, 1H; C^2*H*, coord. Np), 5.13 (m, 1H; cod C*H*=CH *trans* to P), 5.18 (m, 1H; NC*H*CH$_3$, free Np), 5.44 (m, 1H; cod C*H*=CH), 6.34 (m, 1H; C^8*H*, coord. Np), 6.47 (d, $^3J_{H,H}$ = 5.5 Hz, 1H; C^5*H*, coord. Np), 6.52 (t, $^3J_{H,H}$ = 5.3 Hz, 1H; C^7*H*, coord. Np), 6.68 (d, $^3J_{H,H}$ = 5.4 Hz, 1H; C^3*H*, coord. Np), 6.73 (t, $^3J_{H,H}$ = 6.0 Hz, 1H; C^6*H*, coord. Np), 7.12 (d, $^3J_{H,H}$ = 7.0 Hz, 1H; binol H), 7.19 (d, $^3J_{H,H}$ = 7.1 Hz, 1H; binol H), 7.20 (m, 1H; binol H), 7.38 (m, 1H; binol H), 7.39 (m, 1H; binol H), 7.48 (m, 1H; binol H), 7.54 (d, $^3J_{H,H}$ = 3.4 Hz, 1H; C^3*H*, free Np), 7.57 (m, 1H; binol H), 7.60 (m, 1H; binol H), 7.66 (m, 1H; binol H), 7.72 (d, $^3J_{H,H}$ = 8.2 Hz, 1H; C^4*H*, free Np), 7.80 (m, 1H; C^6*H*, free Np), 7.82 (m, 1H; C^8*H*, free Np), 7.88 (d, $^3J_{H,H}$ = 8.5 Hz, 1H; C^2*H*, free Np), 8.05 (d, $^3J_{H,H}$ = 8.2 Hz, 1H; binol H), 8.07 (m, 1H; C^7*H*, free Np), 8.10 (d, $^3J_{H,H}$ = 9.0 Hz, 1H; binol H), 8.14 (d, $^3J_{H,H}$ = 8.4 Hz, 1H; binol H), 8.29 ppm (m, 1H; C^5*H*, free Np); ^{13}C NMR (176 MHz, $CDCl_3$, −40 °C): δ = 21.9 (free NCH*C*H$_3$), 24.6 (cod *C*H$_2$CH=CH), 25.5 (coord. NCH*C*H$_3$), 27.1 (cod *C*H$_2$CH=CH), 32.8 (cod *C*H$_2$CH=CH), 37.8 (cod *C*H$_2$CH=CH), 50.4 (d, $^2J_{P,C}$ = 23.3 Hz, coord. N*C*HCH$_3$), 50.8 (d, $^2J_{P,C}$ = 21.8 Hz, free N*C*HCH$_3$), 58.7 (C^1, coord. Np), 55.0 (C^4, coord. Np), 82.3 (C^2, coord. Np), 88.4 (cod CH$_2$*C*H=CH), 89.1 (cod CH$_2$*C*H=CH), 89.4 (binol), 89.5 (cod CH$_2$*C*H=CH), 89.3 (binol), 89.9 (C^5, coord. Np), 94.3 (C^3, coord. Np), 96.3 (C^7, coord. Np), 98.6 (C^8, coord. Np), 98.7 (binol), 98.8 (C^6, coord. Np), 98.9 (binol), 102.2 (cod CH$_2$*C*H=CH), 104.8 (binol), 117.9 (C^{8a}, coord. Np), 120.3 (C^{4a}, coord. Np), 120.5 (C^8, free Np), 120.6 (C^5, free Np), 120.7 (C^6, free Np), 121.5 (C^7, free Np), 121.3 (binol), 121.9 (binol), 122.0 (binol), 125.3 (binol), 124.5 (C^4, free Np), 126.9 (binol), 127.0 (binol), 127.2 (binol), 127. 5 (C^{4a}, free Np), 127.8 (C^{8a}, free Np), 128.3 (C^3, free Np), 128.4 (binol), 128.7 (binol), 128.9 (binol), 129.2 (C^2, free Np), 129.3 (binol), 131.7 (binol), 133.2 (binol), 136.7 (C^1, free Np), 145.0 (binol), 146.2 ppm (binol). Additionally, the ^{13}C NMR signals of the bis[1-(1-naphthyl)ethyl]amino moiety are summarized in Scheme 7. ^{31}P{^{1}H} NMR (121 Hz, $CDCl_3$): δ = 111.9 ppm (s).

(*aR*,*R*,*R*)-[Ir(cod)(1a′,κP)$_2$]SbF$_6$ (4a′): [IrCl(cod)]$_2$ (100.0 mg, 0.15 mmol) and ligand (*aR*,*R*,*R*)-**1a′** (321.2 mg, 0.6 mmol) were dissolved in CH_2Cl_2 (1 mL), and the resulting bright orange solution was stirred at room temperature during 1 h. Then, $AgSbF_6$ (204.6 mg, 0.6 mmol) was added, and the resulting red mixture was stirred vigorously for 2 h. After filtration and evaporation of the solvent, the crude product was washed with diethyl ether and pentane, and the resulting red powder was dried in a vacuum. Yield: 164.8 mg, 34%; ^{1}H NMR (700 MHz, CD_2Cl_2, −40 °C); δ = 0.71 (br. s, 6H; NCHC*H*$_3$), 1.49 (br. s, 6H; NCHC*H*$_3$), 1.80 (m, 2H; CH$_2$, cod C*H*H′), 1.96 (m, 2H; CH$_2$, cod C*H*H′), 2.04 (m, 2H; CH$_2$, cod C*H*H′), 2.21 (m, 2H; CH$_2$, cod C*H*H′), 3.61 (s, 2H; cod C*H*=CH), 5.37 (s, 2H; cod C*H*=CH), 4.45 (m, 2H; NC*H*CH$_3$), 4.86 (m, 2H; NC*H*CH$_3$), 6.14 (s, 2H; binol H), 6.39 (s, 2H; binol H), 6.95 (d, $^3J_{H,H}$ = 8.95 Hz, 2H; binol H), 6.99 (m, 2H; binol H), 7.07 (d, $^3J_{H,H}$ = 8.7 Hz, 2H; binol H), 7.12 (m, 4H; *para* C*H*, Ph), 7.16 (d, $^3J_{H,H}$ = 8.6 Hz, 2H; binol H), 7.29 (t, $^3J_{H,H}$ = 7.2 Hz, 8H; *meta* C*H*, Ph), 7.33 (m, 8H; *ortho* C*H*, Ph), 7.58 (t, $^3J_{H,H}$ = 7.4 Hz, 2H; binol H), 7.94 (d, $^3J_{H,H}$ = 8.8 Hz, 2H; binol H), 8.01 (d, $^3J_{H,H}$ = 7.8 Hz, 2H; binol H), 8.13 (d, $^3J_{H,H}$ = 8.1 Hz, 2H; binol H), 8.21 (d, $^3J_{H,H}$ = 8.8 Hz, 2H; binol H), 8.35 ppm (d, $^3J_{H,H}$ = 8.8 Hz, 2H; binol H); ^{13}C NMR (176 MHz, CD_2Cl_2, −40 °C): δ = 19.7 (free NCH*C*H$_3$), 20.2 (free NCH*C*H$_3$), 25.70 (cod *C*H$_2$CH=CH), 35.57 (cod *C*H$_2$CH=CH), 52.12 (d, $^2J_{P,C}$ = 19.5 Hz, free N*C*HCH$_3$), 55.39 (d, $^2J_{P,C}$ = 24.9 Hz, free N*C*HCH$_3$), 120.39 (binol), 122.21 (binol), 122.77 (binol), 126.05 (binol), 126.3 (4C, *ortho* C, Ph), 126.48 (binol), 126.5 (4C, *meta* C, Ph), 126.59 (binol), 126.65 (4C, *ortho* C, Ph), 126.67 (binol), 126.99 (binol), 127.05 (4C, *meta* C, Ph), 127.14 (binol), 127.18 (binol), 127.2 (binol), 127.45 (4C, *para* C, Ph), 127.99 (binol), 128.19 (4C, *para* C, Ph), 128.81 (binol), 130.94 (cod CH$_2$*C*H=CH), 131.45 (cod CH$_2$*C*H=CH), 131.61 (binol), 131.98 (binol), 132.87 (binol), 139.73 (binol), 141.34 (4C, *ipso* C, Ph), 142.5 (4C, *ipso* C, Ph), 142.81 (binol), 146.06 (binol), 147.91 ppm (binol); ^{31}P{^{1}H} NMR (283 MHz, CD_2Cl_2): δ = 132.2 ppm (s); HRMS (MALDI): *m*/*z*: calcd for $C_{80}H_{72}N_2O_4P_2Ir$: 1379.4591; found: 1379.4607 $[M-SbF_6]^+$; elemental analysis calcd for $C_{80}H_{72}N_2O_4F_6P_2SbIr$: C 59.48, H 4.49, N 1.73; found: C 59.40, H 4.54, N 1.41.

(*aS*,*S*,*S*)-[Ir(cod)(1b′,κP)$_2$]SbF$_6$ (4b′): [IrCl(cod)]$_2$ (100 mg, 0.15 mmol) and ligand (*aR*,*R*,*R*)-**1b′** (321.2 mg, 0.6 mmol) were dissolved in CD_2Cl_2 (1 mL), and the resulting bright orange solution was stirred at room temperature during 1 h. Then, $AgSbF_6$ (204.6 mg, 0.6 mmol) was added, and the resulting red mixture was stirred vigorously for 2 h. After filtration the ^{31}P NMR spectrum of the reaction solution showed a singlet at δ = 128.6 ppm and a second signal at δ = 13.2 ppm in a 1:1 ratio, which we were unable to assign. After 10 min of reaction time, the signal at δ = 128.6 ppm disappeared, and the peak at δ = 13.2 ppm was the only signal in the ^{31}P NMR spectrum. The chemical shift of δ = 128.6 ppm is close to that of the cationic disubstituted complex (*aR*,*R*,*R*)-**4a′** (δ = 132.2 ppm). This suggests that the primary product is an unstable bis(phosphoramidite) complex that rapidly decomposes.

Asymmetric cyclopropanation: Catalyst preparation: [IrCl(cod)]$_2$ (120 μmol) and the ligand (either 230 or 460 μmol, 2 or 4 equiv, see Table 2) were dissolved in CH_2Cl_2 (2 mL). After stirring for 1 h, $AgSbF_6$ (230 μmol) was added, and the red slurry was stirred vigorously for 2 h. After isolating AgCl by filtration, the solvent was partially evaporated (1 mL), and Et_2O was added. The resulting red precipitate was washed twice with diethyl ether and pentane and dried in a vacuum overnight. The isolated cationic complexes (24 μmol) were dissolved in freshly dis-

tilled CH_2Cl_2, and styrene (480 μmol, 55 μL) and decane (internal standard for GC analysis, 80 μL) were added. Then a solution of distilled ethyl diazoacetate (480 μmol, 50 μL) in CH_2Cl_2 (1 mL) was added over 6 h by syringe pump. The solution was stirred for an additional 14 h. The catalytic reaction of the corresponding naphthyl complexes was carried out by following the same procedure. All catalytic runs were performed twice and gave the same results within experimental error. The olefin conversion and cyclopropane yield (as a sum of the *cis* and *trans* isomers) were determined by GC analysis after filtration over silica to remove the catalyst.

Acknowledgements

We thank Dr. Igor S. Mikhel for preliminary experiments concerning complexes **2a** and **3a**, Pietro Butti and Katrin Niedermann (ETH Zürich) for the X-ray structures of **2a** and **2b′**, and the Swiss National Science Foundation for financial support to T.O. (grant no. 200020-119848).

[1] Recent relevant review articles: a) T. Jerphagnon, M. G. Pizzuti, A. J. Minnaard, B. L. Feringa, *Chem. Soc. Rev.* **2009**, *38*, 1039–1075; b) K. L. Ding, Z. B. Han, Z. Wang, *Chem. Asian J.* **2009**, *4*, 32–41; c) C. A. Falciola, A. Alexakis, *Eur. J. Org. Chem.* **2008**, 3765–3780; d) M. T. Reetz, *Angew. Chem.* **2008**, *120*, 2592–2626; *Angew. Chem. Int. Ed.* **2008**, *47*, 2556–2588; e) G. Erre, S. Enthaler, K. Junge, S. Gladiali, M. Beller, *Coord. Chem. Rev.* **2008**, *252*, 471–491; f) A. J. Minnaard, B. L. Feringa, L. Lefort, J. G. De Vries, *Acc. Chem. Res.* **2007**, *40*, 1267–1277; g) F. López, A. J. Minnaard, B. L. Feringa, *Acc. Chem. Res.* **2007**, *40*, 179–188.

[2] G. Helmchen, A. Dahnz, P. Dubon, M. Schelwies, R. Weihofen, *Chem. Commun.* **2007**, 675–691.

[3] D. Markovic, J. F. Hartwig, *J. Am. Chem. Soc.* **2007**, *129*, 11680–11681, and references therein.

[4] See also: a) D. Polet, A. Alexakis, K. Tissot-Croset, C. Corminboeuf, K. Ditrich, *Chem. Eur. J.* **2006**, *12*, 3596–3609; b) I. Lyothier, C. Defieber, E. M. Carreira, *Angew. Chem.* **2006**, *118*, 6350–6353; *Angew. Chem. Int. Ed.* **2006**, *45*, 6204–6207.

[5] L. Eberhardt, D. Armspach, J. Harrowfield, D. Matt, *Chem. Soc. Rev.* **2008**, *37*, 839–864.

[6] B. Bartels, C. Garcia-Yebra, G. Helmchen, *Eur. J. Org. Chem.* **2003**, 1097–1103.

[7] R. Shintani, H. Nakatsu, K. Takatsu, T. Hayashi, *Chem. Eur. J.* **2009**, *15*, 8692–8694.

[8] a) D. Huber, A. Mezzetti, *Tetrahedron: Asymmetry* **2004**, *15*, 2193–2197; b) D. Huber, P. G. A. Kumar, P. S. Pregosin, A. Mezzetti, *Organometallics* **2005**, *24*, 5221–5223; c) D. Huber, P. G. A. Kumar, P. S. Pregosin, I. S. Mikhel, A. Mezzetti, *Helv. Chim. Acta* **2006**, *89*, 1696–1715.

[9] I. S. Mikhel, H. Rüegger, P. Butti, F. Camponovo, D. Huber, A. Mezzetti, *Organometallics* **2008**, *27*, 2937–2948.

[10] For a review on secondary interactions in asymmetric hydrosilylation, see: S. E. Gibson, M. Rudd, *Adv. Synth. Catal.* **2007**, *349*, 781–795.

[11] Selected papers on MAP, MOP, and related ligands: a) G. C. Lloyd-Jones, S. C. Stephen, M. Murray, C. P. Butts, S. Vyskocyl, P. Kocovsky, *Chem. Eur. J.* **2000**, *6*, 4348–6357; b) Y. Wang, X. Li, J. Sun, K. L. Ding, *Organometallics* **2003**, *22*, 1856–1862; c) P. G. A. Kumar, P. Dotta, R. Hermatschweiler, P. S. Pregosin, A. Albinati, S. Rizzato, *Organometallics* **2005**, *24*, 1306–1314; d) J. W. Faller, N. Sarantopoulos, *Organometallics* **2004**, *23*, 2008–2014.

[12] Selected papers on bidentate σ,1,2-η-arylalkyl ligands: a) H. Ossor, M. Pfeffer, J. T. B. H. Jastrzebski, C. H. Stam, *Inorg. Chem.* **1987**, *26*, 1169–1171; b) C. S. Li, C. H. Cheng, F. L. Liao, S. L. Wang, *J. Chem. Soc. Chem. Commun.* **1991**, 710–712; c) C. S. Li, D. C. Jou, C. H. Cheng, *Organometallics* **1993**, *12*, 3945–3954; d) K. R. Reddy, K. Surekha, G. H. Lee, S. M. Peng, S. T. Liu, *Organometallics* **2001**, *20*, 5557–5563; e) M. Catellani, C. Mealli, E. Motti, P. Paoli, E. Perez-Carreno, P. S. Pregosin, *J. Am. Chem. Soc.* **2002**, *124*, 4336–4346.

[13] a) S. H. Bergens, P. H. Leung, B. Bosnich, A. L. Rheingold, *Organometallics* **1990**, *9*, 2406–2408; b) N. M. Brunkan, M. R. Gagne, *Organometallics* **2002**, *21*, 4711–4717.

[14] a) T. E. Barder, S. D. Walker, J. R. Martinelli, S. L. Buchwald, *J. Am. Chem. Soc.* **2005**, *127*, 4685–4696; b) W. J. Marshall, V. V. Grushin, *Organometallics* **2003**, *22*, 555–562; c) S. M. Reid, R. C. Boyle, J. T. Mague, M. J. Fink, *J. Am. Chem. Soc.* **2003**, *125*, 7816–7817; d) J. Yin, M. P. Rainka, X. X. Zhang, S. L. Buchwald, *J. Am. Chem. Soc.* **2002**, *124*, 1162–1163.

[15] Recent papers: a) T. E. Barder, *J. Am. Chem. Soc.* **2006**, *128*, 898–904; b) U. Christmann, D. A. Pantazis, J. Benet-Buchholz, J. E. McGrady, F. Maseras, R. Vilar, *J. Am. Chem. Soc.* **2006**, *128*, 6376–6390; c) P. Dotta, P. G. A. Kumar, P. S. Pregosin, A. Albinati, S. Rizzato, *Organometallics* **2004**, *23*, 4247–4254.

[16] a) B. Bartels, C. Garcia-Yebra, F. Rominger, G. Helmchen, *Eur. J. Inorg. Chem.* **2002**, 2569–2586; b) F. Giacomina, A. Meetsma, L. Panella, L. Lefort, A. H. M. de Vries, J. G. de Vries, *Angew. Chem.* **2007**, *119*, 1519–1522; *Angew. Chem. Int. Ed.* **2007**, *46*, 1497–1500.

[17] M. Ahlmann, O. Walter, *J. Organomet. Chem.* **2004**, *689*, 3117–3131.

[18] C. M. Thomas, R. Mafua, B. Therrien, E. Rusanov, H. Stoeckli-Evans, G. Suss-Fink, *Chem. Eur. J.* **2002**, *8*, 3343–3352.

[19] S. Filipuzzi, P. S. Pregosin, M. J. Calhorda, P. J. Costa, *Organometallics* **2008**, *27*, 2949–2958.

[20] E. L. Muetterties, J. R. Bleeke, E. J. Wucherer, T. A. Albright, *Chem. Rev.* **1982**, *82*, 499–525.

[21] a) N. P. D. Thi, S. Spichiger, P. Paglia, G. Bernardinelli, E. P. Kündig, P. L. Timms, *Helv. Chim. Acta* **1992**, *75*, 2593–2607; b) E. P. Kündig, C. Perret, P. S. Spichiger, G. Bernardinelli, *J. Organomet. Chem.* **1985**, *286*, 183–200.

[22] G. Zhu, K. E. Janak, J. S. Figueroa, G. Parkin, *J. Am. Chem. Soc.* **2006**, *128*, 5452–5461.

[23] a) M. Bosch, M. Laubender, B. Weberndörfer, H. Werner, *Chem. Eur. J.* **1999**, *5*, 2203–2211; b) M. Bosch, K. Ilg, H. Werner, *Eur. J. Inorg. Chem.* **2001**, 3181–3185.

[24] M. Ichinose, H. Suematsu, T. Katsuki, *Angew. Chem.* **2009**, *121*, 3167–3169; *Angew. Chem. Int. Ed.* **2009**, *48*, 3121–3123.

[25] a) A. Demonceau, F. Simal, A. F. Noels, C. Vias, R. Nunez, F. Teixidor, *Tetrahedron Lett.* **1997**, *38*, 7879; b) B. Cetinkaya, I. Ozdemir, P. H. Dixneuf, *J. Organomet. Chem.* **1997**, *534*, 153–158.

[26] I. Saltsman, L. Simkhovich, Y. Balazs, I. Goldberg, Z. Gross, *Inorg. Chim. Acta* **2004**, *357*, 3038–3046.

[27] M. P. Doyle in *Catalytic Asymmetric Synthesis* (Ed.: I. Ojima), Wiley-VCH, Weinheim, **2000**, p. 193.

[28] J. L. Herde, J. C. Lambert, C. V. Senoff, *Inorganic Synthesis*, Wiley, New York, **1974**, pp. 18–20.

[29] MEXICO: McMaster program for exchange line-shape calculations, Version 3, A. D. Bain.

Received: September 4, 2009
Revised: October 28, 2009
Published online: December 9, 2009

